Electronic Supplementary Material (ESI) for Nanoscale.

Electronic Supplementary Information

2D Bismuthene via Acid-Intercalated Exfoliation Showing Strong Nonlinear Near-infrared Responses for Mode-locking Lasers

*Qi-Qi Yang,[a] Rui-Tong Liu,[a] Chao Huang,[b] Yi-Fan Huang [c], Lin-Feng Gao,[a] Bing Sun,[a] Zhi-Peng Huang,[a] Lei Zhang,[a] Chen-Xia Hu,[a] Ze-Qi Zhang,[a] Chun-Lin Sun,[a] Qiang Wang,[a] * Yu-Long Tang [b] * and Hao-Li Zhang [a] **

a State Key Laboratory of Applied Organic Chemistry (SKLAOC), Key Laboratory of Nonferrous Metal Chemistry and Resources Utilization of Gansu Province, College of Chemistry and Chemical Engineering, Key Laboratory of Special Function Materials and Structure Design, Ministry of Education, Lanzhou University, Lanzhou, 730000, China

b Key Laboratory for Laser Plasmas (Ministry of Education), Department of Physics and Astronomy, Collaborative Innovation Center of IFSA, Shanghai Jiao Tong University, Shanghai, 200240, China

c Science and Technology on Material Performance Evaluating in Space Environment Laboratory, Lanzhou Institute of Physics, Lanzhou, 730000, China

1. The optimizing of the reaction conditions

(1) **Table S1**: Quantity optimization of $(NH_4)_2S_2O_8$ and H_2O_2 for the intercalation.

Sample Number	**$(NH_4)_2S_2O_8$**	**30% H_2O_2**	**Product quantity (Absorption @ 785 nm)**	**Crystalline quality (XRD observation)**
1	0.66 mmol	0	0.214	Poor, and mixed products
2	**0.66 mmol**	**200 μl (1.98 mmol)**	**0.208**	**good (this work)**
3	2.00 mmol	0	0.175	poor
4	2.00 mmol	200 μl (1.98 mmol)	0.128	poor
5	0.10 mmol	200 μl (1.98 mmol)	0.174	poor
Conclusion	*H_2SO_4, $(NH_4)_2S_2O_8$, H_2O_2 are all indispensable for the exfoliation and function as intercalant, oxidizing agent and gas bubbling agent, respectively. *The molar ratio of the relevant reagents needs to be optimized. With the quantity of H_2SO_4 (18.40 mmol, significantly excessive) and bulk Bi (0.14 mmol) fixed, $(NH_4)_2S_2O_8$ and H_2O_2 are the two ingredients significantly influencing the product quality.			

(2)

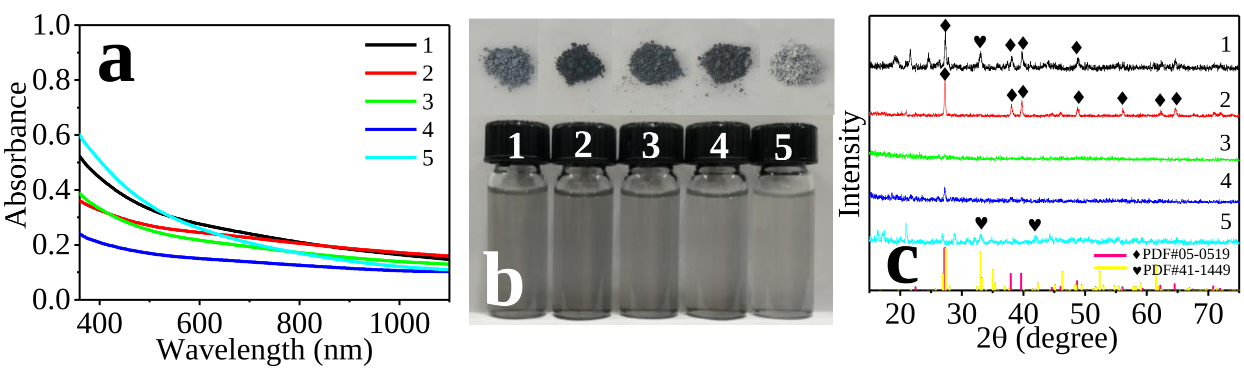

Figure S1. (a) The UV-Vis-NIR spectra of the as-prepared 2D Bi nanosheets; the corresponding digital photos: dried powders (upper) and samples in NMP solution (lower). (b) and XRD patterns (c). PDF card (#05-0519) is from Bi and (#41-1449) is from Bi_2O_3.

2. More SEM images with different resolution

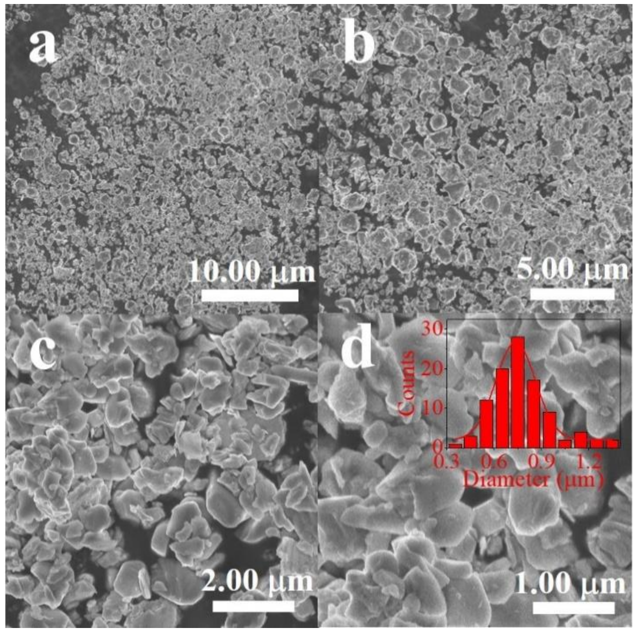

Figure S2. More SEM images with different resolution confirmed the overall uniform flat structure of the exfoliated Bi nanosheets with lateral size of 735± 297 nm based on the statistical data of 100 flakes.

3. More representative AFM images

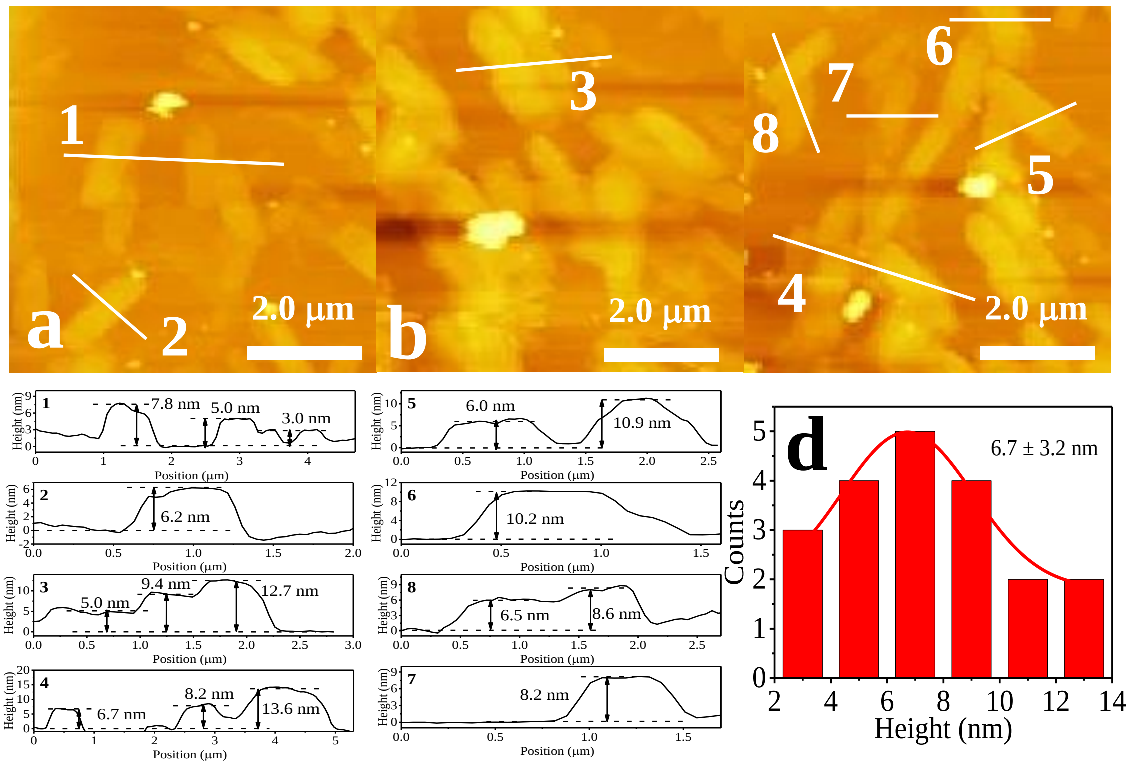

Figure S3. More representative AFM images verified the few layers thickness of the exfoliated Bi nanosheets. Typical thickness was ± nm based on the statistical data of 20 flakes.

4. More representative TEM images

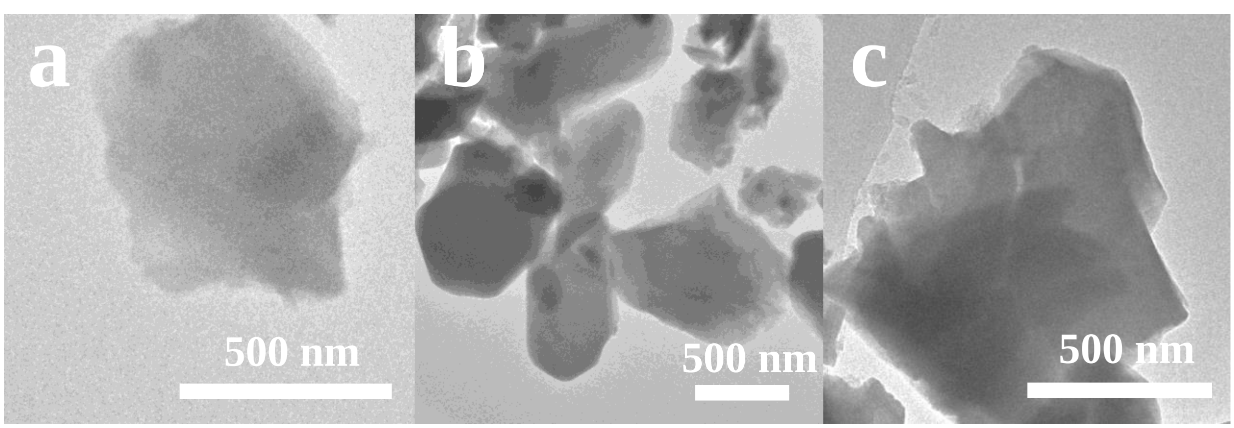

Figure S4. More representative TEM images of the Bi nanosheets.

5. The Z-scan experimental setup and data processing procedures. [1-4]

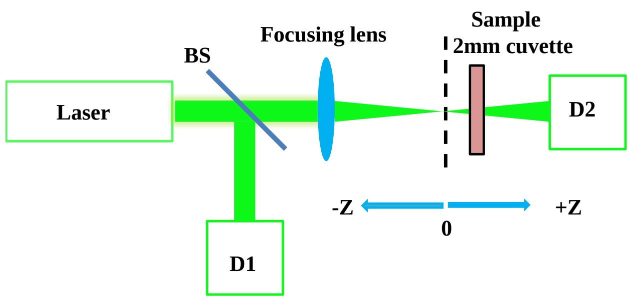

Figure S5. Schematic illustration of the Z-scan setup. D1 and D2 are photodetectors.

(1) The Z-scan setup: The setup comprise of a Q-switched Nd:YAG laser (Continuum, Model Surelite SL-I-10), optical elements and photodetectors. The laser has two output wavelength of 532 nm and 1064 nm, with a FWHM of ~4 ns and a repetition rate of 10 Hz. The temporal and spatial profiles of the output pulses were customized with an approximate Gaussian distribution. The radius of optical spot at the focus point was about 40 μm.

(2) Data fitting procedures: The Z-scan data were fitted to the nonlinear transmission equation using a sum of two nonlinear absorptions with opposite signs:

$$\alpha(I) = \frac{\alpha_0}{1 + \frac{I}{I_S}} + \beta I$$

eq. (S1)

where $\alpha(I)$ is the total nonlinear absorption coefficient, α_0 is the linear absorption coefficient, β is the negative nonlinear absorption coefficient, I is the incident laser intensity and Is is the saturation intensity, defined as the laser intensity at which α_0 drops to 50% of its initial value.

6. More open aperture Z-scan data under various laser pulse power.

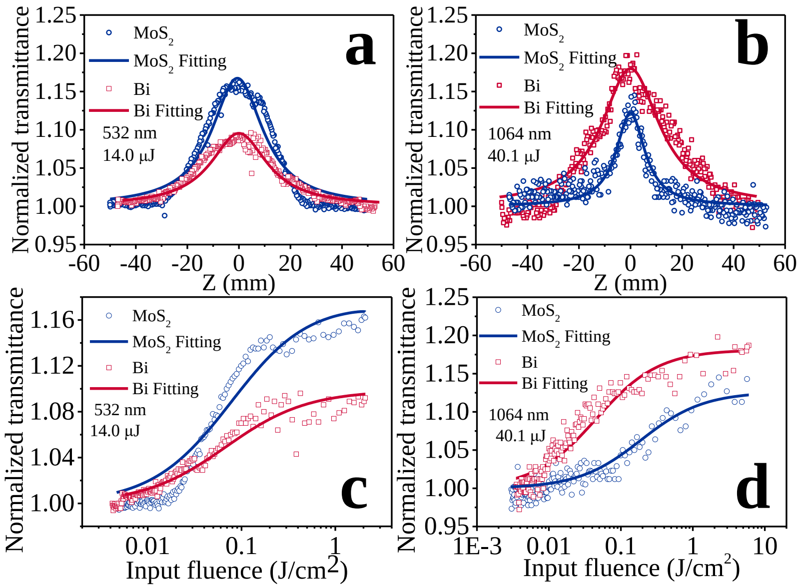

Figure S6. Open aperture Z-scan data (symbols) and fitted curves (solid curves) for the samples with a similar linear transmittance of ~0.70 in NMP at the excitation of 532 nm, 14.0 μJ (a) and 1064 nm, 40.1 μJ (b), and the corresponding plots of transmittance versus input fluence (c) and (d), respectively.

7. Table S2. Summary of the fitted nonlinear optical parameters for the samples.

Samples	λ_{laser} **(nm)**	E_{laser} **(μJ)**	T	β **(m/W)**	I_S **(W/m²)**
Bi	532	4.6	0.69	-2.1×10^{-10}	1.4×10^{12}
MoS_2	532	4.6	0.70	-2.4×10^{-10}	1.1×10^{12}
Bi	532	14.0	0.68	-1.2×10^{-10}	3.0×10^{12}
MoS_2	532	14.0	0.68	-1.6×10^{-10}	1.7×10^{12}
Bi	1064	11.2	0.68	-3.9×10^{-10}↑	7.3×10^{11}
MoS_2	1064	11.2	0.67	-3.3×10^{-11}	9.4×10^{12}
Bi	1064	40.1	0.69	-1.4×10^{-10}↑	2.1×10^{12}
MoS_2	1064	40.1	0.68	-4.7×10^{-11}	6.5×10^{12}

8. 3D plot of the transient absorption spectra in the NIR region.

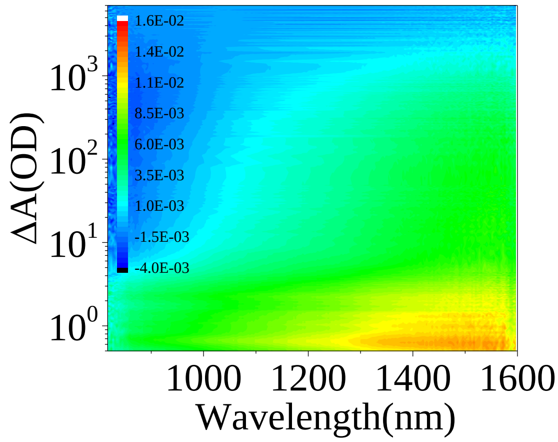

Figure S7. 3D plot (wavelength vs. time vs. intensity) of the transient absorption spectra in the NIR region for the Bi nanosheets in NMP solvent (0.32 O.D. at 400 nm in a 2 mm-cuvette) pumped at 400 nm.

9. fs transient absorption spectra of Bi nanosheets pumped at 350 nm.

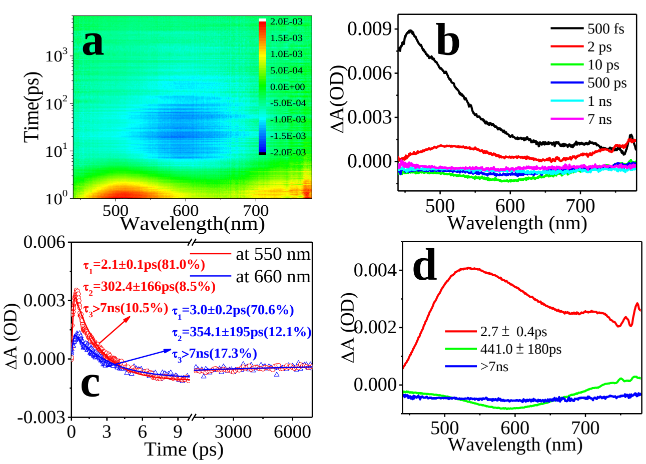

Figure S8. fs transient absorption spectra of Bi nanosheets in NMP solvent (0.36 O.D. at 400 nm in a 2 mm-cuvette) pumped at 350 nm: The 3D plot (a); Selected spectra at different time delays (b); Representative decay curves recorded at 550 nm and 660 nm (c); The spectral characteristic features obtained with the global fitting algorithm (d).

10. fs transient absorption spectra of Bi nanosheets pumped at 800 nm.

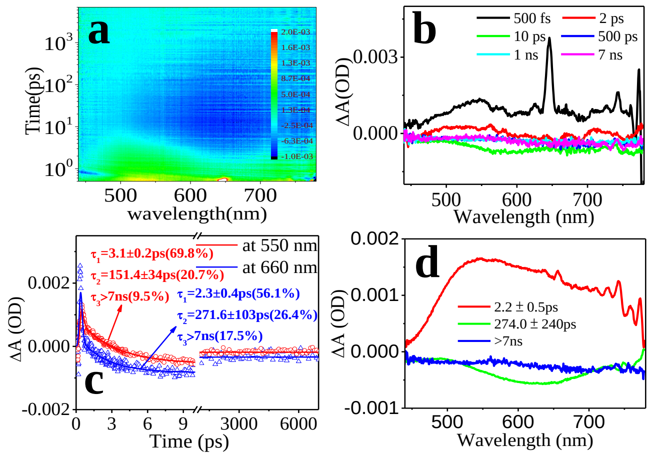

Figure S9. fs transient absorption spectra of Bi nanosheets in NMP solvent (0.22 O.D. at 400 nm in a 2 mm-cuvette) pumped at 800 nm: The 3D plot (a); Selected spectra at different time delays (b); Representative decay curves recorded at 550 nm and 660 nm (c); The spectral characteristic features obtained with the global fitting algorithm (d).

Reference

1. M. Zhao, M. J. Chang, Q. Wang, Z. T. Zhu, X. P. Zhai, M. Zirak, A. Z. Moshfegh, Y. L. Song and H. L. Zhang, *Chem. commun.*, 2015, **51**, 12262-12265.
2. M. Zhao, K. Liu, Y.-D. Zhang, Q. Wang, Z.-G. Li, Y.-L. Song and H.-L. Zhang, *Mater. Horiz.*, 2015, **2**, 619-624.
3. M. Zhao, R. Peng, Q. Zheng, Q. Wang, M. J. Chang, Y. Liu, Y. L. Song and H. L. Zhang, *Nanoscale*, 2015, **7**, 9268-9274.
4. L. F. Gao, J. Y. Xu, Z. Y. Zhu, C. X. Hu, L. Zhang, Q. Wang and H. L. Zhang, *Nanoscale*, 2016, **8**, 15132 -15136.